Near-Infrared Light-Responsive Hybrid Hydrogels for Synergistic Chemo-Photothermal Therapy of Oral Cancer

Yongzhi Wu[a], Fangman Chen[b], Nengwen Huang[a], Jinjin Li[a], Chenzhou Wu[a], Bowen Tan[a], Yunkun Liu[a], Longjiang Li[a], Chao Yang[b,*], Dan Shao[c], Jinfeng Liao[a,*]

[a] State Key Laboratory of Oral Diseases, National Clinical Research Centre for Oral Diseases, West China Hospital of Stomatology, Sichuan University, Chengdu, 610041, China.

[b] School of Biomedical Sciences and Engineering, South China University of Technology, Guangzhou International Campus, Guangzhou, Guangdong 510006, China

[c] Institutes for Life Sciences, School of Medicine, South China University of Technology, Guangzhou, Guangdong 510006, China

Corresponding author:

Dr. Jinfeng Liao, State Key Laboratory of Oral Diseases, National Clinical Research Centre for Oral Diseases, West China Hospital of Stomatology, Sichuan University, Chengdu, 610041, China. E-mail: liaojinfeng.762@163.com

Dr. Chao Yang, School of Biomedical Sciences and Engineering, South China University of Technology, Guangzhou International Campus, Guangzhou, Guangdong 510006, China. E-mail: chaoyang@scut.edu.cn

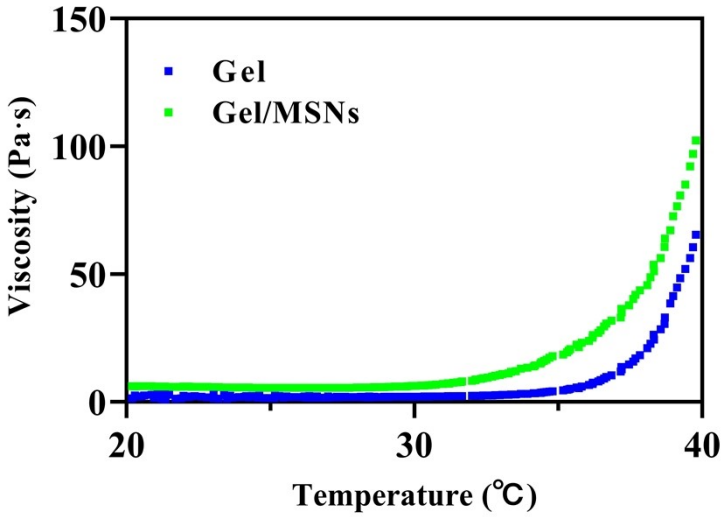

Fig. S1 Dynamic viscosity measurements of Gel and Gel/MSNs.

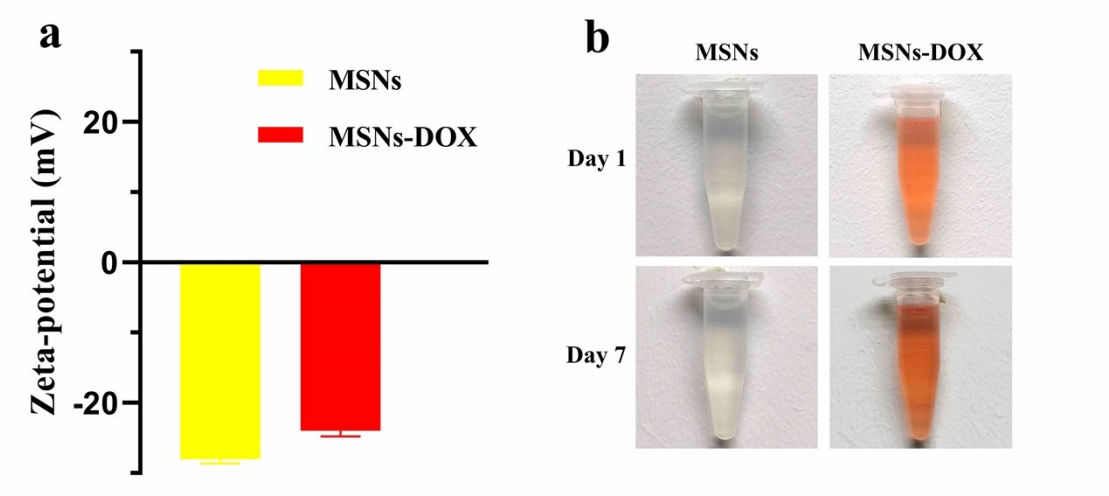

Fig. S2 Characterizations of MSNs and MSNs-DOX. (a) Zeta potential of MSNs and MSNs-DOX dispersed in DI water. (b) The pictures of MSNs and MSNs-DOX dispersed in DI water.

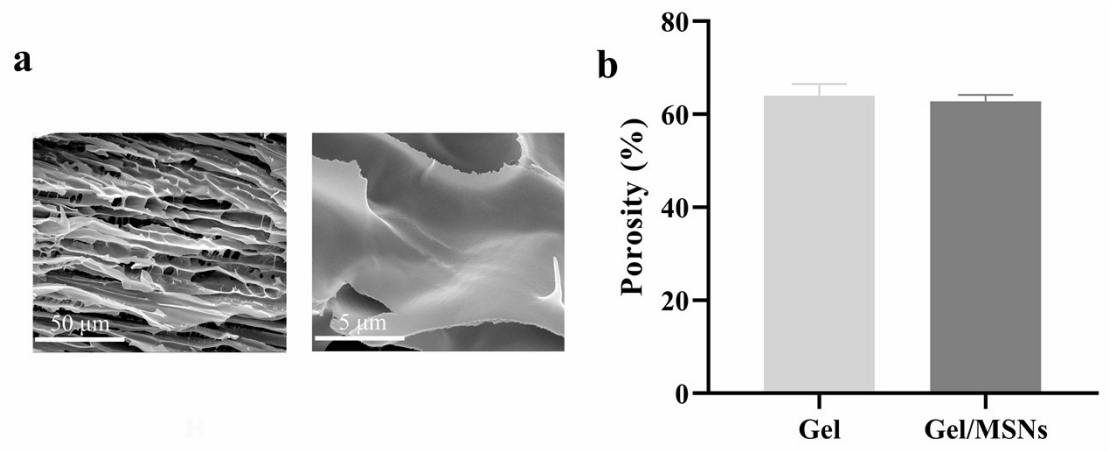

Fig. S3 Morphology characterizations of resulting hydrogels. (a) SEM images of blank gel. (b) The porosities of Gel and Gel/MSNs.

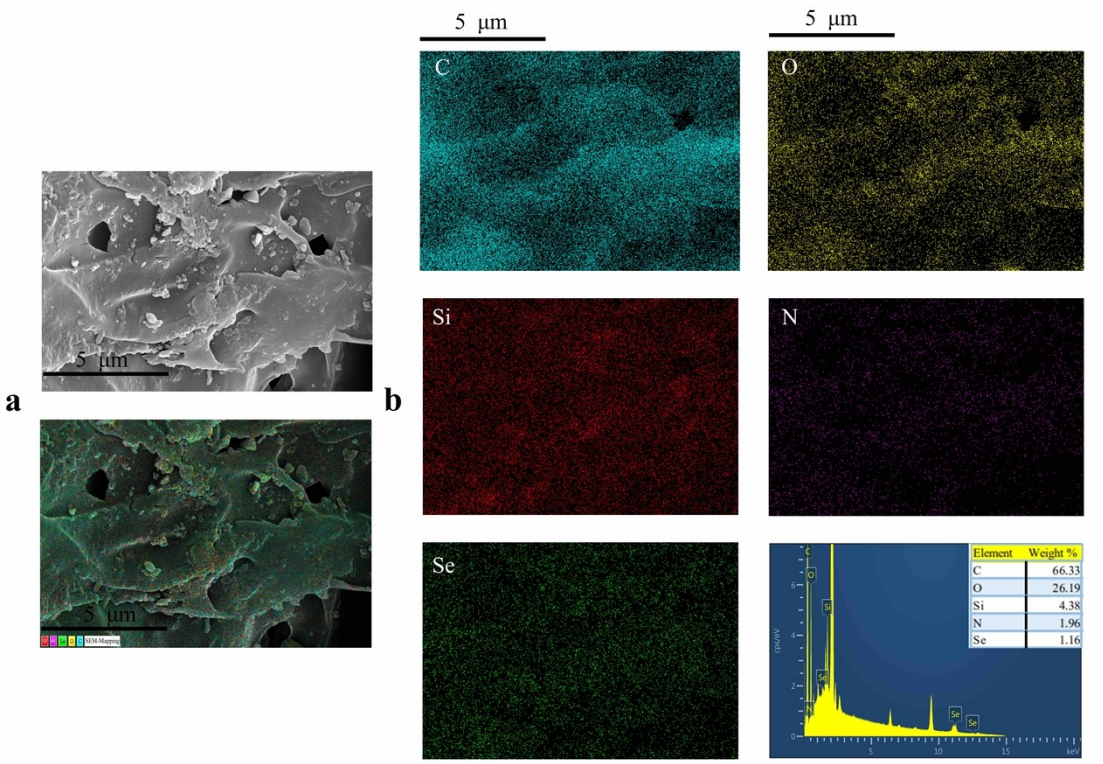

Fig. S4 SEM-mapping and EDS analysis of the MC/MSNs hydrogel. (a) The SEM images of Gel/MSNs. (b) Element mapping and weight measurement of the hydrogel.

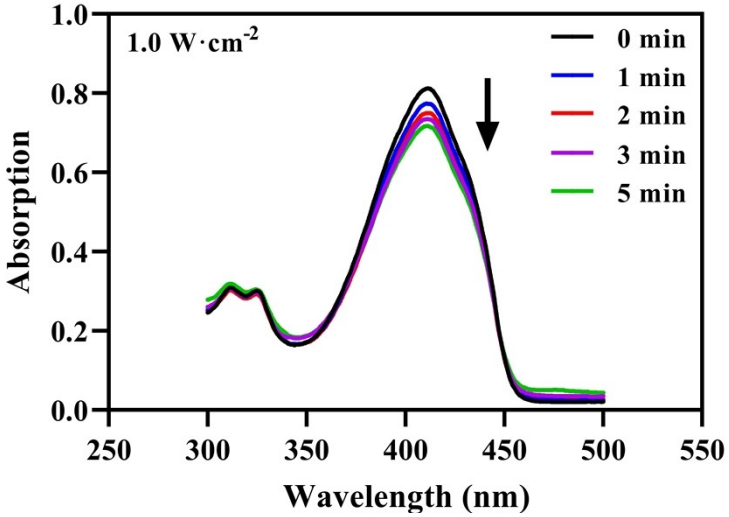

Fig. S5 Decay curves of the absorption of DPBF by singlet oxygen generated from Gel/IR820 under 1.0 W·cm^{-2} irradiation at 808 nm.

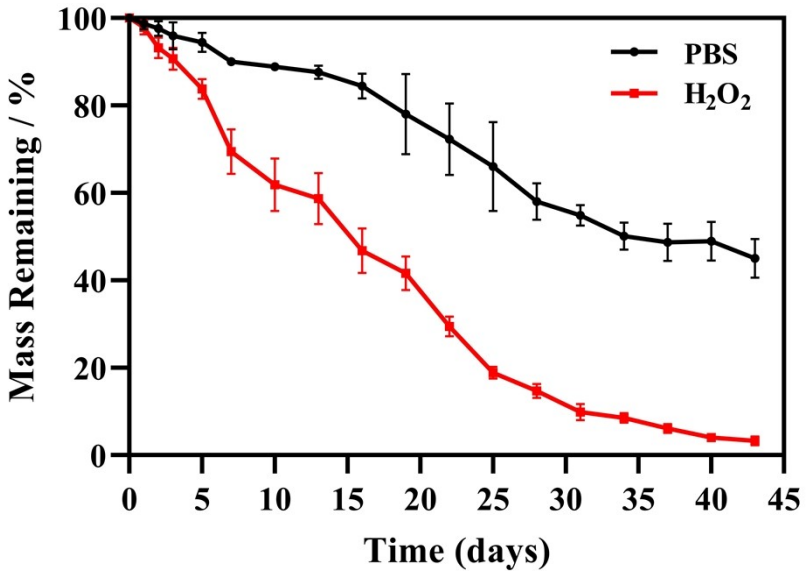

Fig. S6 *In vitro* degradation of Gel/MSNs in different mediums.

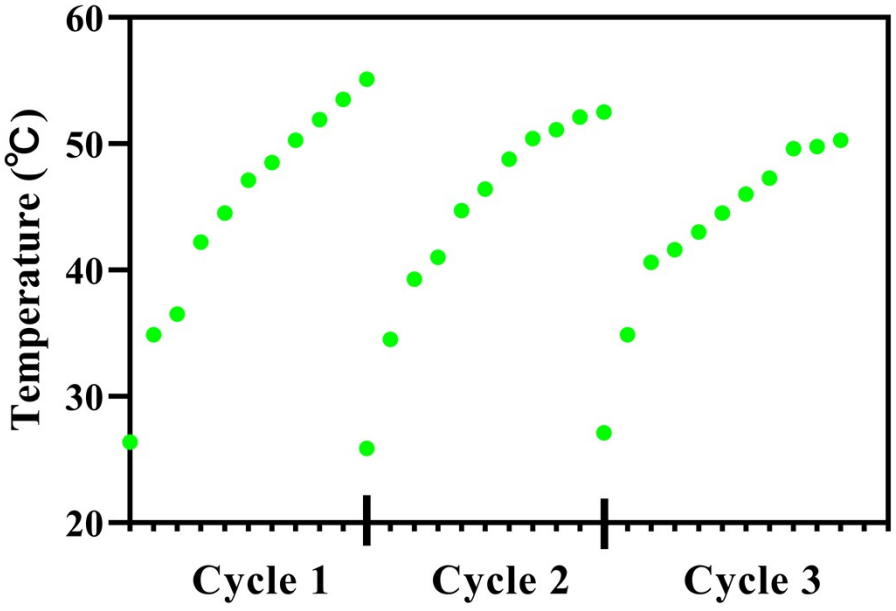

Fig. S7 Temperature profiles of IR820-loaded hydrogel (200 μg/mL) subjected to three cycles of NIR irradiation (2.0 $W \cdot cm^{-2}$).

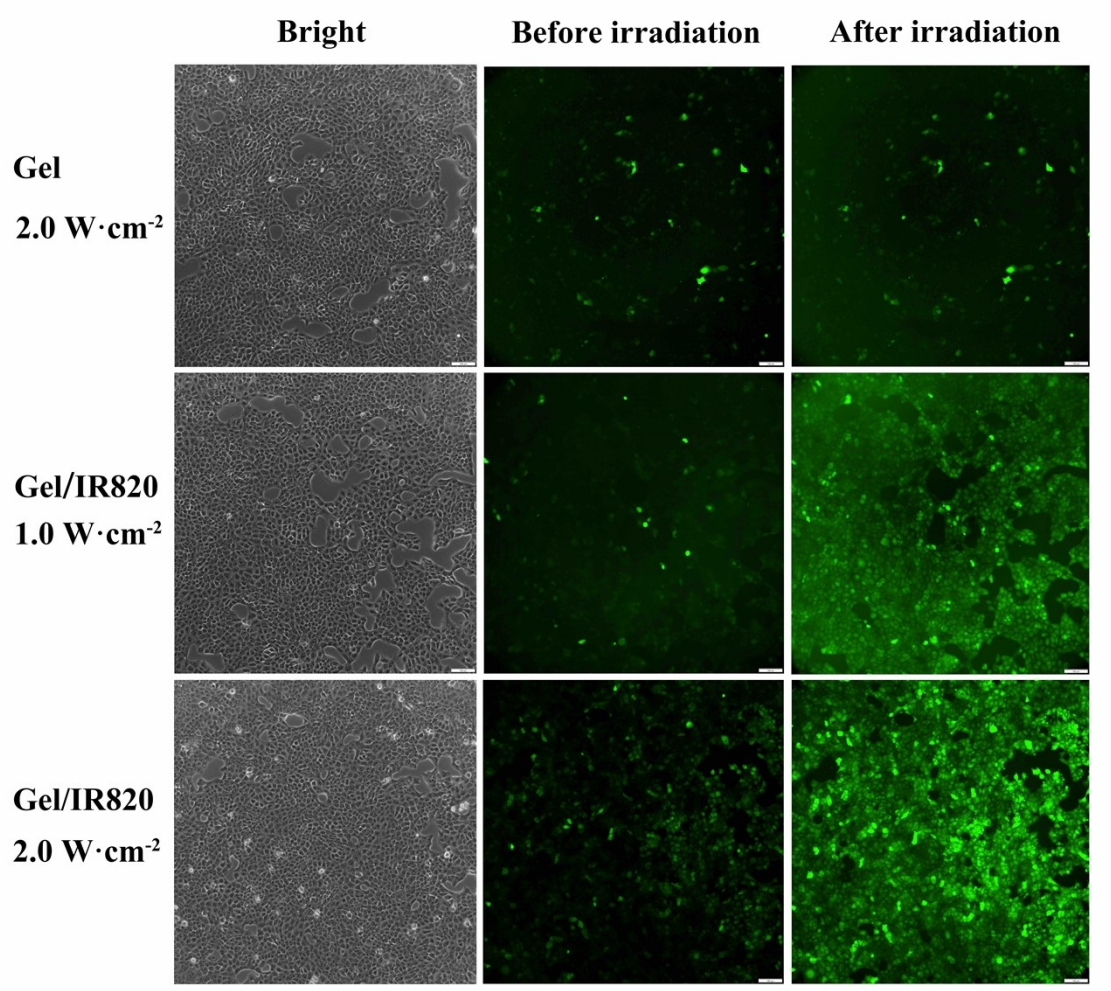

Fig. S8 Fluorescence images of ROS generation in Cal27 cells with incubation of IR820-containing Gel before and after irradiation; scale bar 100 μm.

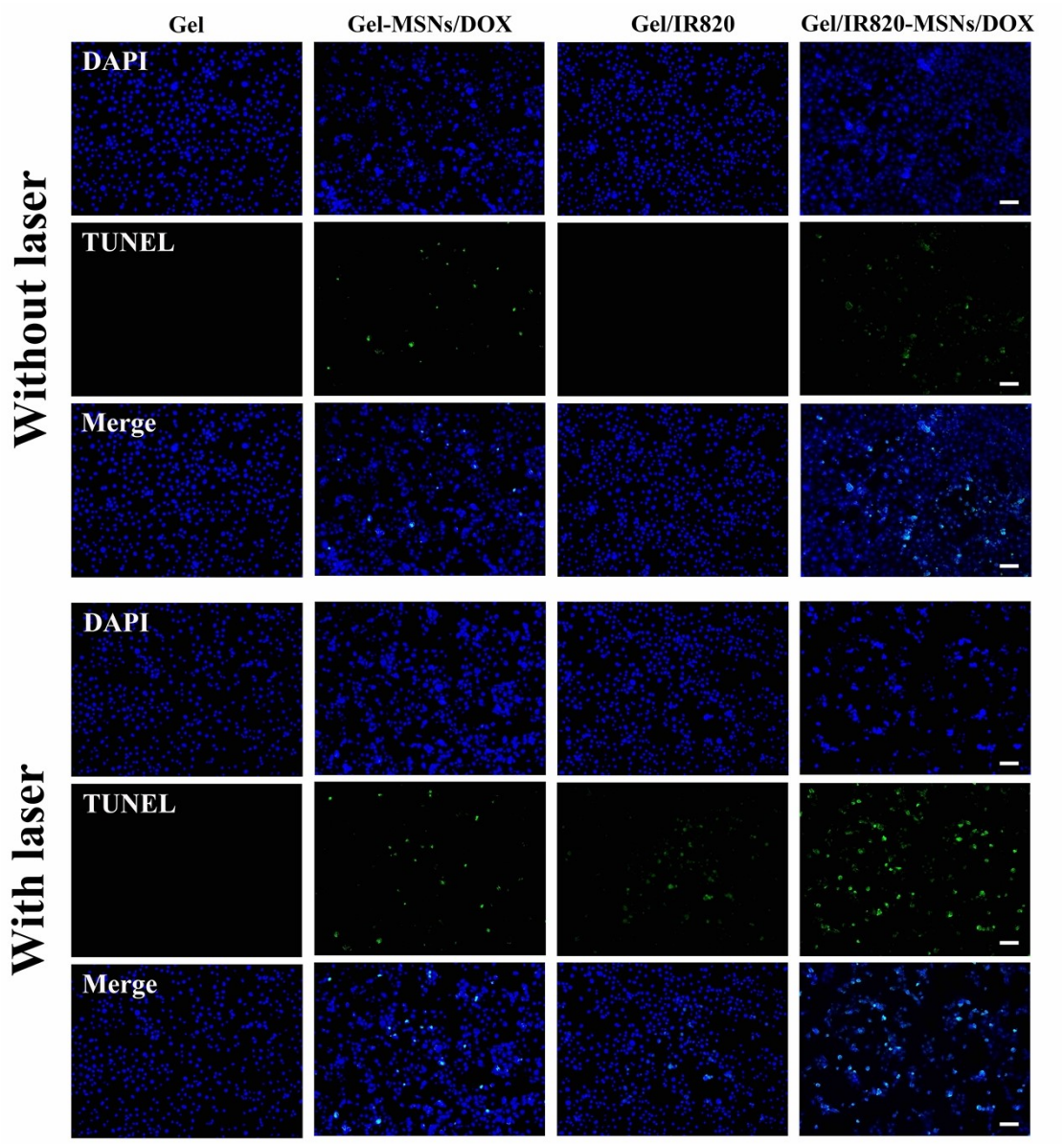

Fig. S9 Assessment of the apoptosis of Cal27 cells under indicated treatments by TUNEL assay.

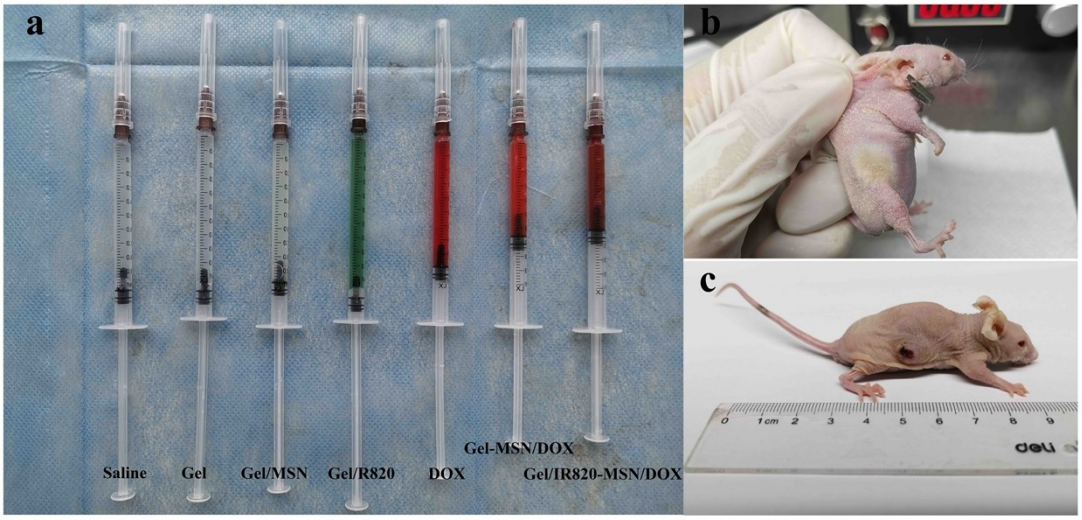

Fig. S10 *In vivo* photo-chemo therapy. (a) Photos of the injectable formulations. Photos of tumor-bearing mice after NIR irradiation at (b) 2 h and (c) day 3 in G7.